MHD Flow past a Semi-Infinite Vertical Plate with Mass Transfer

G. Palani[1], **U. Srikanth**[2]

[1]Department of Mathematics
Sri Subramaniyaswamy Govt. Arts College
Tiruttani-631 209, India
gpalani32@yahoo.co.in

[2]Corporation Hr. Sec. School
Chennai-81, India

Abstract. An analysis is performed to study the MHD flow of an electrically conducting, incompressible, viscous fluid past a semi-infinite vertical plate with mass transfer, under the action of transversely applied magnetic field is carried out. The heat due to viscous dissipation and the induced magnetic field are assumed to be negligible. The dimensionless governing equations are unsteady, two-dimensional, coupled and non-linear partial differential equations. A most accurate, unconditionally stable and fast converging implicit finite difference scheme is used to solve the non-dimensional governing equations. The effects of external cooling ($Gr > 0$) of the plate by the free convection are studied.

Keywords: magnetic field, Grashof Number, skin friction, vertical plate.

1 Introduction

The natural convection flows are frequently encountered in nature. They have many applications in Science and Technology. Extensive research work has been published on flow past a vertical plate under different conditions. The analytical method fails to solve the problem of unsteady two-dimensional natural convection flow past a semi-infinite vertical plate. The advent of advanced numerical methods and the developments in computer technology pave the way to solve such difficult problems. Finite difference methods play an important role in solving the partial differential equations. The unsteady natural convection flow past a semi-infinite vertical plate was first solved by Hellums and Churchill [1], using an explicit finite difference method. Gebhart and Pera [2] obtained the steady state solution for natural convection on a vertical plate with variable surface temperature and variable mass diffusion using similarity variables. Callahan and Marner [3] gave a numerical solution for the problem of transient free convection with mass transfer on an isothermal vertical plate by employing an explicit finite difference

scheme. Numerical solution of transient free convection flow with mass transfer on a vertical plate by employing an implicit method was obtained by Soundalgekar and Ganesan [4].

The influence of magnetic field on viscous incompressible fluid of electrically conducting is of importance in many applications such as extrusion of plastics in the manufacture of Rayon and Nylon, purification of crude oil, textile industry etc. In many process industries the cooling of threads or sheets of some polymer materials is of importance in the production line. The rate of cooling can be controlled effectively to achieve final products of desired characteristics by drawing threads etc., in the presence of an electrically conducting fluid subjected to magnetic field.

Soundalgekar et al. [5] analyzed the problem of free convection effects on Stokes problem for a vertical plate under the action of transversely applied magnetic field. Nirmal C. Sacheti et al. [6] obtained an exact solution for unsteady Magneto hydrodynamics free convection flow on an impulsively started vertical plate with constant heat flux. Shanker and Kishan [7] discussed the effect of mass transfer on the MHD flow past an impulsively started vertical plate with variable temperature or constant heat flux. El-bashbeshy [8] studied heat and mass transfer along a vertical plate under the combined buoyancy effects of thermal and species diffusion, in the presence of the magnetic field. Ganesan and Palani [9] obtained numerical solution of Unsteady MHD flow past a semi-infinite isothermal vertical plate. Ganesan and Palani [10] studied numerical solution of transient free convection MHD flow of an incompressible viscous fluid flow past a semi-infinite inclined plate with variable surface heat and mass flux. The set of governing equations are solved by using an implicit finite difference scheme. Orhan Aydin and Ahmet Kaya [11] investigates mixed convection heat transfer about a permeable vertical plate in the presence of magneto and thermal radiation effects, The set of governing equations of the problem are solved using similarity variables. The problem of steady laminar magneto hydrodynamic(MHD) mixed convection heat transfer about a vertical plate is solved numerically by Orhan Aydin and Ahmet Kaya [12] taking into account the effect of ohmic heating and viscous dissipation. In recent years, the effects of the transverse magnetic field on the flow of an incompressible, viscous electrically conducting fluid have also been studied extensively by many research workers. However, unsteady natural convection flow over a semi-infinite vertical plate with MHD with isothermal heat and mass transfer has not been given any attention in the literature. Hence it has been now proposed to solve the transient free convection MHD flow past a semi-infinite isothermal vertical plate with mass transfer by an implicit finite difference scheme.

2 Formulation of the problem

We consider here the unsteady flow of a viscous incompressible fluid past a semi-infinite vertical plate with mass transfer under the influence of transversely applied magnetic field. The x-axis is taken along the plate in the vertically upward direction and the y-axis is chosen perpendicular to the plate at the leading edge as shown in Fig. 1. The origin of x-axis is taken to be at the leading edge of the plate. The gravitational acceleration g is

acting downward. Initially (i.e., at time $t' = 0$), it is assumed that the plate and the fluid are at the same ambient temperature T'_∞ and the species concentration C'_∞. When $t' > 0$, the temperature of the plate and the species concentration is maintained to be T'_w (greater than T'_∞) and C'_w (greater than C'_∞) respectively. It is assumed that the effect of viscous dissipation is negligible in the energy equation. The concentration of the diffusing species in the binary mixture is assumed to be very small in comparison with other chemical species, which are present, and hence we neglect Soret and Duffor effects. There is no chemical reaction between the fluid and the diffusing species. A uniformly transverse magnetic field is applied in the direction of flow. It is further assumed that the interaction of the induced magnetic field with the flow is considered to be negligible compared to the interaction of the applied magnetic field with the flow. The fluid properties are assumed to be constants except for the body force terms in the momentum equations which are approximated by the Boussinesq relations.
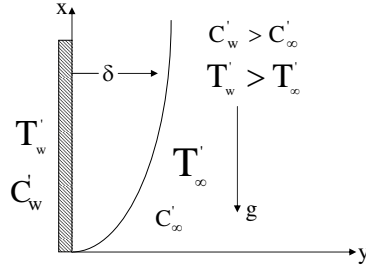

Fig. 1. The physical coordinate system.

Based on these assumptions the continuity, momentum, energy and species equations become [2–4]

$$\frac{\partial u}{\partial x} + \frac{\partial v}{\partial y} = 0, \tag{1}$$

$$\frac{\partial u}{\partial t'} + u\frac{\partial u}{\partial x} + v\frac{\partial u}{\partial y} = g\beta(T' - T'_\infty) + g\beta^*(C' - C'_\infty) + \nu\frac{\partial^2 u}{\partial y^2} - \frac{\sigma B_o^2}{\rho}u, \tag{2}$$

$$\frac{\partial T'}{\partial t'} + u\frac{\partial T'}{\partial x} + v\frac{\partial T'}{\partial y} = \alpha\frac{\partial^2 T'}{\partial y^2}, \tag{3}$$

$$\frac{\partial C'}{\partial t'} + u\frac{\partial C'}{\partial x} + v\frac{\partial C'}{\partial y} = D\frac{\partial^2 C'}{\partial y^2}, \tag{4}$$

where u and v are the velocity components in the x and y directions respectively, C' is the species concentration, D is the coefficient of diffusion in the mixture, T' is the temperature of the fluid in the boundary layer, t' is the time, β is the volumetric coefficient of thermal expansion, β^* is the volumetric coefficient of expansion with concentration, ν is the kinematic viscosity, g is the acceleration due to gravity and α is the thermal diffusivity, ρ is the density of the fluid, B_o^2 is the magnetic field strength and σ is the electrical conductivity of the fluid.

347

The initial and boundary conditions are

$$
\begin{aligned}
t' \le 0: \quad & u = 0, \quad v = 0, \quad T' = T'_\infty \quad C' = C'_\infty, \\
t' > 0: \quad & u = 0, \quad v = 0, \quad T' = T'_w \quad C' = C'_w \quad \text{at } y = 0, \\
& u = 0, \qquad\qquad T' = T'_\infty, \quad C' = C'_\infty \quad \text{at } x = 0, \\
& u \to 0, \qquad\qquad T \to T_\infty, \quad C \to C_\infty \quad \text{as } y \to \infty.
\end{aligned}
\tag{5}
$$

On introducing the following non-dimensional quantities:

$$
\begin{aligned}
& X = \frac{x}{L}, \quad Y = \frac{y}{L} Gr^{1/4}, \quad U = \frac{uL}{\nu} Gr^{-1/2}, \quad V = \frac{vL}{\nu} Gr^{1/4}, \quad t = \frac{\nu t'}{L^2} Gr^{1/2}, \\
& T = \frac{T' - T'_\infty}{T'_w - T'_\infty}, \quad C = \frac{C' - C'_\infty}{C'_w - C'_\infty}, \quad Gr = \frac{g\beta L^3 (T'_w - T'_\infty)}{\nu^2}, \\
& Gc = \frac{g\beta^* L^3 (C'_w - C'_\infty)}{\nu^2}, \quad Pr = \frac{\nu}{\alpha}, \quad Sc = \frac{\nu}{D}, \quad N = \frac{Gc}{Gr}, \quad M = \frac{\sigma B_o^2 L^2}{\rho\nu} Gr^{-1/2}.
\end{aligned}
$$

Here L is the length of the plate, Gr is the Grashof number, Gc is the modified Grashof number, M is the magnetic field parameter, N is the buoyancy ratio parameter, Sc is the Schmidt number and Pr is the Prandtl number.

Equations (1)–(4) are reduced to the following dimensionless form

$$
\frac{\partial U}{\partial X} + \frac{\partial V}{\partial Y} = 0,
\tag{6}
$$

$$
\frac{\partial U}{\partial t} + U\frac{\partial U}{\partial X} + V\frac{\partial U}{\partial Y} = T + NC + \frac{\partial^2 U}{\partial Y^2} - MU,
\tag{7}
$$

$$
\frac{\partial T}{\partial t} + U\frac{\partial T}{\partial X} + V\frac{\partial T}{\partial Y} = \frac{1}{Pr}\frac{\partial^2 T}{\partial Y^2},
\tag{8}
$$

$$
\frac{\partial C}{\partial t} + U\frac{\partial C}{\partial X} + V\frac{\partial C}{\partial Y} = \frac{1}{Sc}\frac{\partial^2 C}{\partial Y^2}.
\tag{9}
$$

The corresponding initial and boundary conditions in dimensionless form are as follows:

$$
\begin{aligned}
t \le 0: \quad & U = 0, \quad V = 0, \quad T = 0, \quad C = 0, \quad \text{for all } Y, \\
t > 0: \quad & U = 0, \quad V = 0, \quad T = 1, \quad C = 1, \quad \text{at } Y = 0, \\
& U = 0, \qquad\qquad T = 0 \quad C = 0, \quad \text{at } X = 0, \\
& U \to 0, \qquad\qquad T \to 0 \quad C \to 0 \quad \text{as } Y \to \infty.
\end{aligned}
\tag{10}
$$

Using the non-dimensional quantities specified in equation 6, the local as well as average values of skin-friction, Nusselt number and Sherwood number in dimensionless form are as follows:

$$
\tau_X = Gr^{3/4}\left(\frac{\partial U}{\partial Y}\right)_{Y=0},
\tag{11}
$$

$$\overline{\tau} = Gr^{3/4} \int\limits_{0}^{1} \left(\frac{\partial U}{\partial Y}\right)_{Y=0} \mathrm{d}X, \tag{12}$$

$$Nu_X = -Gr^{1/4} X \left(\frac{\partial T}{\partial Y}\right)_{Y=0}, \tag{13}$$

$$\overline{Nu} = -Gr^{1/4} \int\limits_{0}^{1} \left(\frac{\partial T}{\partial Y}\right)_{Y=0} \mathrm{d}X, \tag{14}$$

$$Sh_X = -Gr^{1/4} X \left(\frac{\partial C}{\partial Y}\right)_{Y=0}, \tag{15}$$

$$\overline{Sh} = -Gr^{1/4} \int\limits_{0}^{1} \left(\frac{\partial C}{\partial Y}\right)_{Y=0} \mathrm{d}X. \tag{16}$$

The derivatives involved in equations (11) to (16) are evaluated by using a five-point approximation formula and then the integrals are evaluated by Newton-Cotes closed integration formula.

3   Numerical procedure

The two-dimensional, non-linear, unsteady and coupled partial differential equations (7)–(10) under the initial and boundary conditions (11) are solved using an implicit finite difference scheme of Crank-Nicolson type which is fast convergent and unconditionally stable. The finite difference equation corresponding to equations (7)–(10) are given by:

$$\frac{[U_{i,j}^{k+1} - U_{i-1,j}^{k+1} + U_{i,j}^{k} - U_{i-1,j}^{k} + U_{i,j-1}^{k+1} - U_{i-1,j-1}^{k+1} + U_{i,j-1}^{k} - U_{i-1,j-1}^{k}]}{4\Delta X}$$
$$+ \frac{[V_{i,j}^{k+1} - V_{i,j-1}^{k+1} + V_{i,j}^{k} - V_{i,j-1}^{k}]}{2\Delta Y} = 0, \tag{17}$$

$$\frac{[U_{i,j}^{k+1} - U_{i,j}^{k}]}{\Delta t} + U_{i,j}^{k} \frac{[U_{i,j}^{k+1} - U_{i-1,j}^{k+1} + U_{i,j}^{k} - U_{i-1,j}^{k}]}{2\Delta X}$$
$$+ V_{i,j}^{k} \frac{[U_{i,j+1}^{k+1} - U_{i,j-1}^{k+1} + U_{i,j+1}^{k} - U_{i,j-1}^{k}]}{4\Delta Y}$$
$$= \frac{1}{2}[T_{i,j}^{k+1} + T_{i,j}^{k}] + \frac{N}{2}[C_{i,j}^{k+1} + C_{i,j}^{k}]$$
$$+ \frac{[U_{i,j-1}^{k+1} - 2U_{i,j}^{k+1} + U_{i,j+1}^{k+1} + U_{i,j-1}^{k} - 2U_{i,j}^{k} + U_{i,j+1}^{k}]}{2(\Delta Y)^2}$$
$$- \frac{M}{2}[U_{i,j}^{k+1} + U_{i,j}^{k}], \tag{18}$$

$$\frac{[T_{i,j}^{k+1} - T_{i,j}^k]}{\Delta t} + U_{i,j}^k \frac{[T_{i,j}^{k+1} - T_{i-1,j}^{k+1} + T_{i,j}^k - T_{i-1,j}^k]}{2\Delta X}$$

$$+ V_{i,j}^k \frac{[T_{i,j+1}^{k+1} - T_{i,j-1}^{k+1} + T_{i,j+1}^k - T_{i,j-1}^k]}{4\Delta Y}$$

$$= \frac{1}{Pr} \frac{[T_{i,j-1}^{k+1} - 2T_{i,j}^{k+1} + T_{i,j+1}^{k+1} + T_{i,j-1}^k - 2T_{i,j}^k + T_{i,j+1}^k]}{2(\Delta Y)^2}, \tag{19}$$

$$\frac{[C_{i,j}^{k+1} - C_{i,j}^k]}{\Delta t} + U_{i,j}^k \frac{[C_{i,j}^{k+1} - C_{i-1,j}^{k+1} + C_{i,j}^k - C_{i-1,j}^k]}{2\Delta X}$$

$$+ V_{i,j}^k \frac{[C_{i,j+1}^{k+1} - C_{i,j-1}^{k+1} + C_{i,j+1}^k - C_{i,j-1}^k]}{4\Delta Y}$$

$$= \frac{1}{Sc} \frac{[C_{i,j-1}^{k+1} - 2C_{i,j}^{k+1} + C_{i,j+1}^{k+1} + C_{i,j-1}^k - 2C_{i,j}^k + C_{i,j+1}^k]}{2(\Delta Y)^2}. \tag{20}$$

The region of integration is considered as a rectangle with sides $X_{\max} (= 1)$ and $Y_{\max} (= 16)$, where $Y_{\max}$ corresponds to $Y = \infty$, which lies very well outside the momentum, energy and concentration boundary layers. The maximum of Y was chosen as 16 after some preliminary investigations so that the last two of the boundary conditions (11) are satisfied. Here, the subscript i-designates the grid point along the X-direction, j-along the Y-direction and the superscript k along the t-direction. During any one time step, the coefficients $U_{i,j}^k$ and $V_{i,j}^k$ appearing in the difference equations are treated as constants. The values of U, V, T and C are known at all grid points at $t = 0$, from the initial conditions.

The computations of U, V, T and C at time level $(k + 1)$ using the values at previous time level (k) are carried out as follows: The finite difference equation (20) at every internal nodal point on a particular i-level constitute a tridiagonal system of equations. Such a system of equations are solved by Thomas algorithm as described in Carnahan et al. [13]. Thus, the values of C are found at every nodal point for a particular i at $(k + 1)^{th}$ time level. Similarly, the values of T are calculated from equation (20). Using the values of C and T at $(k + 1)^{th}$ time level in the equation 19, the values of U at $(k + 1)^{th}$ time level are found in a similar manner. Thus, the values of C, T and U are known on a particular i-level. Finally, the values of V are calculated explicitly using the Equation (18) at every nodal point on a particular i-level at $(k + 1)^{th}$ time level. This process is repeated for various i-levels. Thus the values of C, T, U and V are known, at all grid points in the rectangular region at $(k + 1)^{th}$ time level.

Computations are carried out until the steady-state is reached. The steady-state solution is assumed to have been reached, when the absolute difference between the values of U, as well as temperature T and concentration C at two consecutive time steps are less than 10^{-5} at all grid points. After experimenting with few sets of mesh sizes, they have been fixed at the level $\Delta X = 0.05$, $\Delta Y = 0.25$, and the time step $\Delta t = 0.01$. In this case, spatial mesh sizes are reduced by 50 % in one direction, then in both directions, and the results are compared. It is observed that, when mesh size is reduced by 50 % in X-direction and Y-direction the results differ in fourth decimal place. Hence, the above

mentioned sizes have been considered as appropriate mesh sizes for calculation. The local truncation error is $O(\Delta t^2 + \Delta Y^2 + \Delta X)$ and it tends to zero as Δt, ΔY, and ΔX tend to zero, which shows that the system is compatible. Also the Crank-Nicholson system is always unconditionally stable. Thus the compatible and stability ensures convergence. Hence, the present employed scheme is always convergent.

4   Discussion of results

In order to ascertain the accuracy of the numerical results, the present study is compared with available solution in the literature. The velocity profiles for $Pr = 0.1$, $Sc = 0.7$, $N = 2.0$, $M = 0.0$ are compared with the available solution of Callahan and Marner [3] using explicit finite difference scheme in Fig. 2. It is observed that the present results are in good agreement with the solution.
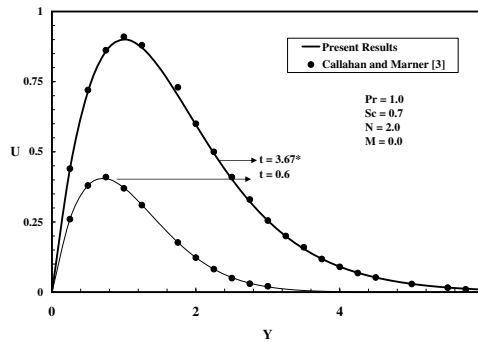
Fig. 2. Comparison velocity profiles at $X = 1.0$ ($*$ – steady state).

Transient velocity profiles are shown in Fig. 3 for different values of buoyancy ratio parameter N and the magnetic field parameter M at the upper edge of the plate viz. at $X = 1.0$. When N increases the combined buoyancy force increases. Therefore velocity increases with N near the plate. Time taken to reach the steady state increases with the increasing value of the magnetic field parameter M. From Fig. 3, we observe that the magnetic parameter M has a retarding effect on velocity. The difference between temporal maximum and steady state decreases marginally as M increases. No temporal maximum is observed for higher values of magnetic field parameter M. The effect of a transverse magnetic field on an electrically conducting fluid give rise to a resistive type force called Lorentz force. This force has tendency to slow down the motion of the fluid and to increases its temperature. To illustrate the effects of Schmidt number and Prandtl number, the steady state velocity distribution near the plate at $X = 1.0$ is presented in Fig. 4. The velocity gradient for air ($Pr = 0.7$) is always greater than the water ($Pr = 7.0$). Physically, this is true because the increase in the Prandtl number is due to increase in the viscosity of the fluid which makes the fluid thick and hence causes a decrease in the velocity of the fluid. An increase in Sc leads to a fall in the velocity. The

transient temperature profile at $X = 1.0$ for different values of N and M are presented in Fig. 5. Temperature increases with the increasing value of the magnetic field parameter M. An increase in N leads to a fall in the temperature. Fig. 6 shows the effect of Sc and Pr on the steady state temperature distribution. Temperature increases as Sc increases. Thermal boundary layer decreases for the larger value of Pr.
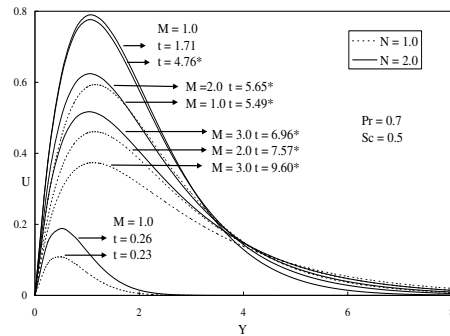

Fig. 3. Transient velocity profiles at $X = 1.0$ for different N and M ($*$ – steady state).
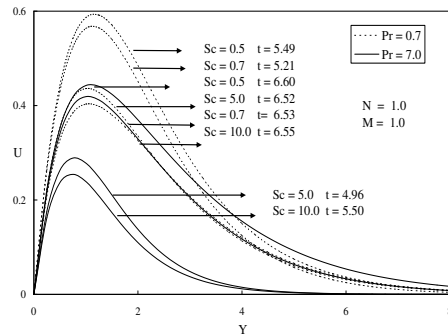
Fig. 4. Steady state velocity profiles at $X = 1.0$ for different Pr and Sc.
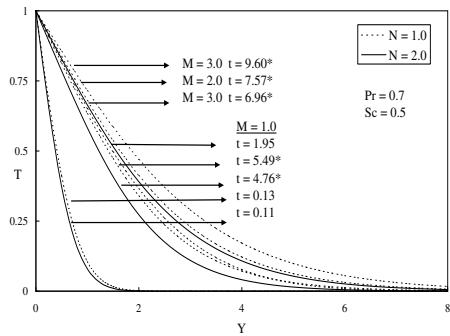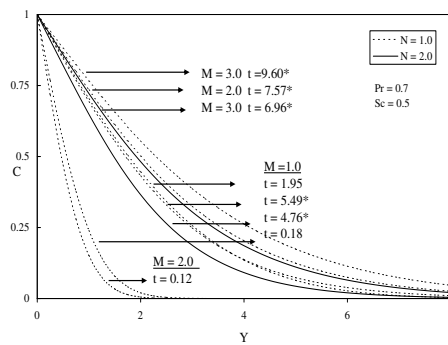

Fig. 5. Transient temperature profiles at $X = 1.0$ for different N and M ($*$ – steady state).
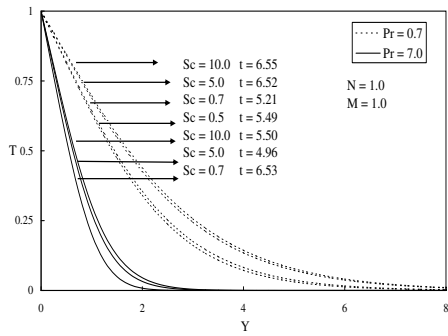
Fig. 6. Steady state temperature profiles at $X = 1.0$ for different Pr and Sc.

Concentration profiles at $X = 1.0$ for different values of buoyancy ratio parameter N and magnetic field parameter M are shown in Fig. 7. The species concentration decreases as N increases. From Fig. 7, we conclude that the transient concentration increases as M increases. In Fig. 8, steady state concentration profiles are plotted for various values of Sc and Pr. As expected concentration is lower for system with larger values of Sc. Species concentration increases with increasing value of Prandtl number of the fluid. In Fig. 9, values of local shear stress are plotted for various values of different values parameter occurring into the problem. As the buoyancy ratio parameter N increases, local skin

friction increases. Local skin friction is reduced by the increasing value of magnetic parameter M, because velocity decreases with the increasing value of M as shown in Fig. 3. The local wall shear stress increases with increasing value of Schmidt number. Also it is observed that local skin friction decreases as Pr increases. In Fig. 10, local Nusselt number i.e., local heat transfer rate is plotted against the axial co-ordinate X at the steady state level. It increases as X increases. Larger values of Nusselt number are observed for higher values of Pr. It decreases as M increases. Also it is observed that local Nusselt number decreases as Sc increases. An increase in N, local Nusselt number is also found to increases.

Fig. 7. Transient concentration profiles at $X = 1.0$ for different N and M ($\ast$ – steady state).
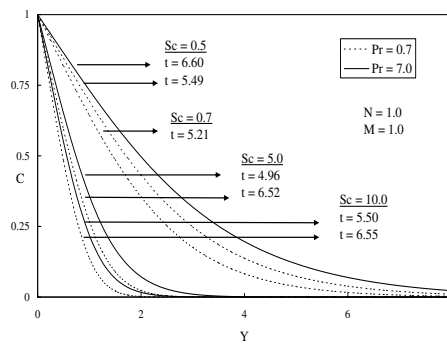

Fig. 8. Steady state concentration profiles at $X = 1.0$ for different Pr and Sc.
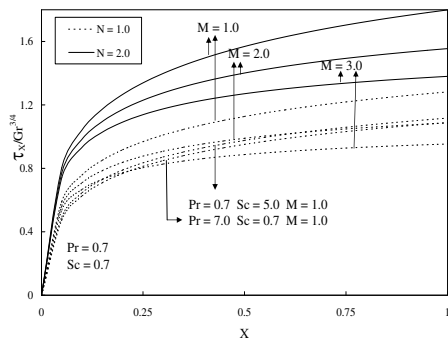

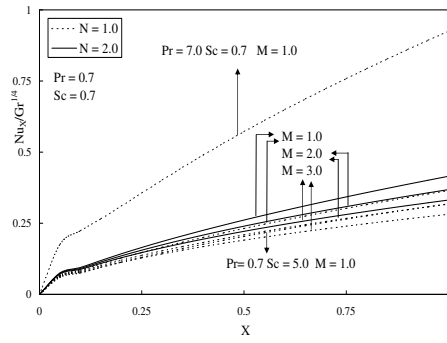Fig. 9. Local skin friction.

Fig. 10. Local Nusselt number.

Steady state local Sherwood number are shown in Fig. 11, for various values of Pr, Sc, N and M. The effect of Sc is greater on the local Sherwood number than any other parameter. It is observed that local Sherwood number decreases as Pr increases. From the figure, we see that localSherwood number increases with the increasing value of N. Average skin friction, average Nusselt number and average Sherwood number are plotted in Figs. 12, 13, 14 respectively for various parameters. Average skin friction decreases

as M or Sc decreases throughout the transient period. Also it is observed that average skin friction increases as N increases. In Fig. 12, the average Nusselt number is same at a particular time level in the initial period for various values of other parameters. This shows that there is only heat conduction in the initial time level. Average Nusselt number decreases as M increases. The same trend is also notice for average Sherwood number. An increase in the value of N, the average Nusselt number increases. The same trend is also observed for average Sherwood number.
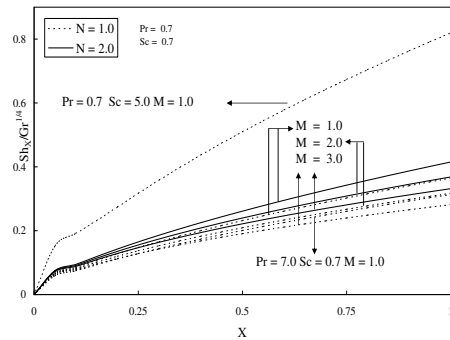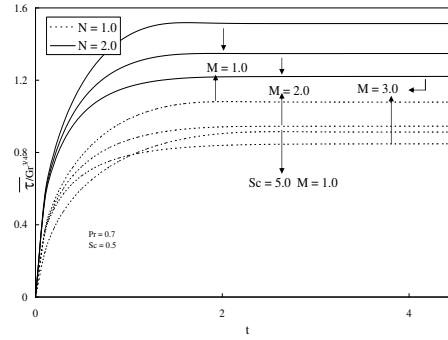

Fig. 11. Local Sherwood number.

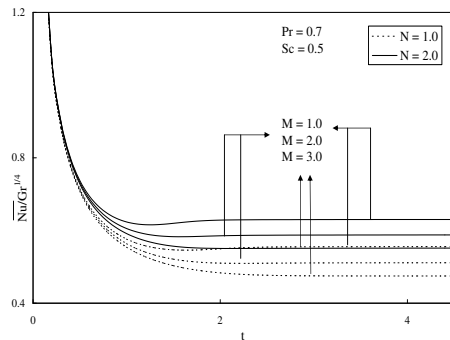Fig. 12. Average skin friction.

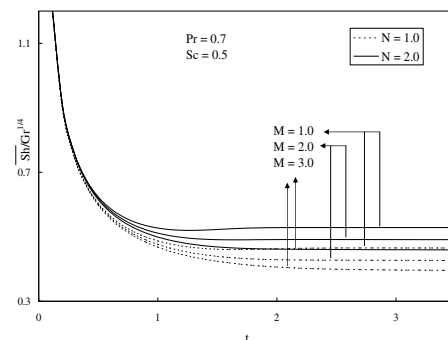Fig. 13. Average Nusselt number.

Fig. 14. Average Sherwood mumber.

5 Conclusions

Finite difference study has been carried out for the flow past a semi-infinite vertical plate with MHD with heat and mass transfer. The dimensionless governing equations are solved by an implicit finite difference scheme of Crank-Nicolson type. A comparison between the present numerical results and available solution is also made. The agreement between the two result is found to be very good. The effect of velocity, temperature, concentration

fields for different parameters are studied. The transient velocity, temperature and concentration profiles all reach maximum values before decreasing slightly to their respective steady-state values. The local as well as average skin-friction, Nusselt number and Sherwood number are shown graphically. The difference between the temporal maximum and steady state decreases marginally as M increases. No temporal maximum is observed for higher values of M. It is observed that the contribution of mass diffusion to the buoyancy force increases the maximum velocity significantly. Local shear stress gets reduced by the increasing value of magnetic field parameter M.

References

1. J. D. Hellums, S. W. Churchill, Transient and steady state free and natural convection, numerical solutions: Part 1. The isothermal vertical plate, *AIChE J.*, **8**, pp. 690–692, 1962.

2. B. Gebhart, L. Pera, The nature of vertical natural convection flows resulting from the combined buoyancy effects of thermal and mass diffusion, *Int. J. Heat Mass Tran.*, **14**, pp. 2025–2050, 1971.

3. G. D. Callahan, W. J. Marner, Transient free convection with mass transfer on an isothermal vertical flat plate, *Int. J. Heat Mass Tran.*, **19**, pp. 165–174, 1976.

4. V. M. Soundalgekar, P. Ganesan, Finite difference analysis of transient free convection with mass transfer on an isothermal vertical flat plate, *Int. J. Eng. Sci.*, **19**, pp. 757–770, 1981.

5. V. M. Soundalgekar, S. K. Gupta, R. N. Aranake, Free convection effects on the MHD Stokes problem for a vertical plate, *Nucl. Eng. Des.*, **51**, pp. 403–407, 1979.

6. N. C. Sacheti, P. Chandran, A. K. Singh, An exact solution for unsteady magnetohydrodynamic free convection flow with constant heat flux, *Int. Commun. Heat Mass*, **29**, pp. 1465–1478, 1986.

7. B. Shanker, N. Kishan, The effects of mass transfer on the MHD flow past an impulsively started infinite vertical plate with variable temperature or constant heat flux, *Journal of Energy, Heat and Mass Transfer*, **19**, pp. 273–278, 1997.

8. E. M. A. Elbashbeshy, Heat and Mass transfer along a vertical plate with variable surface tension and concentration in the presence of magnetic field, *Int. J. Eng. Sci.*, **34**(5), pp. 515–522, 1997.

9. P. Ganesan, G. Palani, Numerical solution of unsteady MHD flow past a semi-infinite isothermal vertical plate, in: *Proceedings of the 6th ISHMT/ASME Head and Mass Transfer Conference and 17th National Heat and Mass Transfer Conference, January 5–7, 2004, Kalpakkam, India*, pp. 184–187, 2004.

10. P. Ganesan, G. Palani, Finite difference analysis of unsteady natural convection MHD flow past an inclined plate with variable surface heat and mass flux, *Int. J. Heat Mass Tran.*, **47**, pp. 4449–4457, 2004.

11. O. Aydin, A. Kaya, Radiation effect on MHD mixed convection flow about a permeable vertical plate, *Heat Mass Transfer*, **45**, pp. 239–246, 2008.

12. O. Aydin, A. Kaya, MHD mixed convection of a viscous dissipating fluid about a permeable vertical flat plate, *Appl. Math. Model.*, **33**(11), pp. 4086–4096, 2009.

13. B. Carnahan, H. A. Luther, J. O. Wilkes, *Applied Numerical Methods*, John Wiley and Sons, New York, 1969.